

# Utility metric for unsupervised feature selection

**Amalia Villa** <sup>Corresp., 1</sup>, **Abhijith Mundanad Narayanan** <sup>1</sup>, **Sabine Van Huffel** <sup>1</sup>, **Alexander Bertrand** <sup>1</sup>, **Carolina Varon** <sup>1,2,3</sup>

<sup>1</sup> Department of Electrical Engineering (ESAT), STADIUS Center for Dynamical Systems, Signal Processing and Data Analytics, KU Leuven, Leuven, Belgium

<sup>2</sup> e-Media Research Lab, Department of Electrical Engineering, KU Leuven, Leuven, Belgium

<sup>3</sup> Circuits and Systems (CAS) group, Delft University of Technology, Delft, The Netherlands

Corresponding Author: Amalia Villa

Email address: amalia.villagomez@kuleuven.be

Feature selection techniques are very useful approaches for dimensionality reduction in data analysis. They provide interpretable results by reducing the dimensions of the data to a subset of the original set of features. When the data lack annotations, unsupervised feature selectors are required for their analysis. Several algorithms for this aim exist in the literature, but despite their large applicability, they can be very inaccessible or cumbersome to use, mainly due to the need for tuning non-intuitive parameters and the high computational demands.

In this work, a publicly available ready-to-use unsupervised feature selector is proposed, with comparable results to the state-of-the-art at a much lower computational cost. The suggested approach belongs to the methods known as spectral feature selectors. These methods generally consist of two stages: manifold learning and subset selection. In the first stage, the underlying structures in the high-dimensional data are extracted, while in the second stage a subset of the features is selected to replicate these structures. This paper suggests two contributions to this field, related to each of the stages involved. In the manifold learning stage, the effect of non-linearities in the data is explored, making use of a radial basis function (RBF) kernel, for which an alternative solution for the estimation of the kernel parameter is presented for cases with high-dimensional data. Additionally, the use of a backwards greedy approach based on the least-squares utility metric for the subset selection stage is proposed.

The combination of these new ingredients results in the Utility metric for Unsupervised feature selection (U2FS) algorithm. The proposed U2FS algorithm succeeds in selecting the correct features in a simulation environment. In addition, the performance of the method on benchmark datasets is comparable to the state-of-the-art, while requiring less computational time. Moreover, unlike the state-of-the-art, U2FS does not require any tuning of parameters.

# 1 Utility metric for unsupervised feature 2 selection

3 **Amalia Villa<sup>1</sup>, Abhijith Mundanad Narayanan<sup>1</sup>, Sabine Van Huffel<sup>1</sup>,**  
4 **Alexander Bertrand<sup>1</sup>, and Carolina Varon<sup>1,2</sup>**

5 <sup>1</sup>**Department of Electrical Engineering (ESAT), STADIUS Center for Dynamical Systems,**  
6 **Signal Processing and Data Analytics, KU Leuven, Leuven, Belgium**

7 <sup>2</sup>**e-Media Research Lab, Department of Electrical Engineering, KU Leuven, Leuven,**  
8 **Belgium**

9 Corresponding author:

10 Amalia Villa<sup>1</sup>

11 Email address: amalia.villagomez@kuleuven.be

## 12 ABSTRACT

13 Feature selection techniques are very useful approaches for dimensionality reduction in data analysis.  
14 They provide interpretable results by reducing the dimensions of the data to a subset of the original set of  
15 features. When the data lack annotations, unsupervised feature selectors are required for their analysis.  
16 Several algorithms for this aim exist in the literature, but despite their large applicability, they can be very  
17 inaccessible or cumbersome to use, mainly due to the need for tuning non-intuitive parameters and the  
18 high computational demands.

19 In this work, a publicly available ready-to-use unsupervised feature selector is proposed, with comparable  
20 results to the state-of-the-art at a much lower computational cost. The suggested approach belongs to the  
21 methods known as spectral feature selectors. These methods generally consist of two stages: manifold  
22 learning and subset selection. In the first stage, the underlying structures in the high-dimensional data  
23 are extracted, while in the second stage a subset of the features is selected to replicate these structures.  
24 This paper suggests two contributions to this field, related to each of the stages involved. In the manifold  
25 learning stage, the effect of non-linearities in the data is explored, making use of a radial basis function  
26 (RBF) kernel, for which an alternative solution for the estimation of the kernel parameter is presented for  
27 cases with high-dimensional data. Additionally, the use of a backwards greedy approach based on the  
28 least-squares utility metric for the subset selection stage is proposed.

29 The combination of these new ingredients results in the Utility metric for Unsupervised feature selection  
30 (U2FS) algorithm. The proposed U2FS algorithm succeeds in selecting the correct features in a simulation  
31 environment. In addition, the performance of the method on benchmark datasets is comparable to the  
32 state-of-the-art, while requiring less computational time. Moreover, unlike the state-of-the-art, U2FS does  
33 not require any tuning of parameters.

## 34 INTRODUCTION

35 Many applications of data science require the study of highly multi-dimensional data. A high number of  
36 dimensions implies a high computational cost as well as a large amount of memory required. Furthermore,  
37 this often leads to problems related to the curse of dimensionality (Verleysen and François, 2005) and thus,  
38 to irrelevant and redundant data for machine learning algorithms (Maindonald et al., 2007). Therefore, it  
39 is crucial to perform dimensionality reduction before analyzing the data.

40 There are two types of dimensionality reduction techniques. On the one hand, feature selection, where  
41 the aim is to keep a subset of the original features. On the other hand, transformation techniques define  
42 a new smaller set of features, which are derived from a combination of all features of the original set.  
43 Some examples of these are Principal Component Analysis (PCA) (Wold et al., 1987) and Independent  
44 Component Analysis (ICA) (Jiang et al., 2006). These methods lead to less interpretable results, in which  
45 the direct relationship between the features and the results is lost.

46 In this work, the focus is on unsupervised feature selectors. Since these methods do not rely on the  
47 availability of labels or annotations in the data, the information comes from the learning of the underlying

48 structure of the data. Despite this challenge, the generalization capabilities of these methods are typically  
49 better than for supervised or semi-supervised methods (Guyon and Elisseeff, 2003).

50 One specific type of unsupervised feature selectors are those based on manifold and sparse learning  
51 (Lunga et al., 2013). These type of methods rely on graph theory to learn the underlying structures of the  
52 data. However, to the best of our knowledge, none explores specifically the behavior of these methods  
53 with data presenting non-linear relationships between the features (i.e., dimensions). While the graph  
54 definition step can make use of kernels to tackle non-linearities, these can be heavily affected by the curse  
55 of dimensionality, since they are often based on a distance metric (Aggarwal et al., 2001).

56 After the manifold learning stage, sparse regression is applied to score the relevance of the features  
57 in the structures present in the graph. These formulations make use of sparsity-inducing regularization  
58 techniques to provide the final subset of features selected, and thus, they are highly computationally  
59 expensive. These methods are often referred to as structured sparsity-inducing feature selectors (SSFS)  
60 (Gui et al., 2016).

61 Despite the large amount of unsupervised SSFS algorithms described in the literature, these methods  
62 are cumbersome to use for a novice user. This is not only due to the codes not being publicly available,  
63 but also due to the algorithms requiring regularization parameters which are difficult to tune, in particular  
64 in unsupervised settings.

65 In this work, an efficient unsupervised feature selector based on the utility metric (U2FS) is proposed.  
66 U2FS is a ready-to-use, publicly available<sup>1</sup> unsupervised feature selector designed to be robust for data  
67 containing non-linearities. The main contributions of this work are:

- 68 • The definition of a new method to automatically approximate the radial-basis function (RBF) kernel  
69 parameter without the need for a user-defined tuning parameter. This method is used to tackle the  
70 curse of dimensionality when embedding the data taking non-linearities into account.
- 71 • The suggestion of a backwards greedy approach for the stage of subset selection, based on the  
72 utility metric for the least-squares problem. The utility metric was proposed in the framework of  
73 supervised learning (Bertrand, 2018), and has been used for channel selection in applications such  
74 as electroencephalography (EEG) (Narayanan and Bertrand, 2020), sensor networks (Szurley et al.,  
75 2014), and microphone arrays (Szurley et al., 2012). Nevertheless, this is the first work in which  
76 this type of approach is proposed for the sparsity-inducing stage of feature selection.
- 77 • Propose a non-parametric and efficient unsupervised SSFS algorithm. This work analyzes the  
78 proposed method U2FS in terms of its complexity, and of its performance on simulated and  
79 benchmark data. The goal is to reduce the computational cost while maintaining a comparable  
80 performance with respect to the state-of-the-art.

81 The rest of the paper is structured as follows. In Related Work, previous algorithms on SSFS are  
82 summarized. In Methods, the proposed U2FS method is described: first the manifold learning stage,  
83 together with the algorithm proposed for the selection of the kernel parameter; and further on, the utility  
84 metric is discussed and adapted to feature selection. The experiments performed in simulations and  
85 benchmark databases, as well as the results obtained are described in the Results and Discussion sections.  
86 Finally, the last section provides some conclusions.

## 87 RELATED WORK

88 Spectral feature selection methods have become widely used in unsupervised learning applications for  
89 high-dimensional data. This is due to two reasons. On the one hand, the use of manifold learning  
90 guarantees the preservation of local structures present in the high-dimensional data. Additionally, its  
91 combination with feature selection techniques not only reduces the dimensionality of the data, but also  
92 guarantees interpretability.

93 Spectral feature selectors learn the structures present in the data via connectivity graphs obtained in  
94 the high-dimensional space (Yan et al., 2006). The combination of manifold learning and regularization  
95 techniques to impose sparsity, allows to select a subset of features from the original dataset that are able  
96 to describe these structures in a smaller dimensional space.

<sup>1</sup>U2FS code can be found in <https://github.com/avillago/u2fs>

97 Most of these algorithms can also be categorized as sparsity-inducing feature selectors, since they  
98 make use of sparsity-inducing regularization approaches to stress those features that are more relevant for  
99 data separation. The sparsity of these approaches is controlled by different statistical norms ( $l_{r,p}$ -norms),  
100 which contribute to the generalization capability of the methods, adapting them to binary or multi-class  
101 problems (Gui et al., 2016). One drawback of these sparse regression techniques is that generally, they  
102 rely on optimization methods, which are computationally expensive.

103 The Laplacian Score (He et al., 2006) was the first method to perform spectral feature selection in an  
104 unsupervised way. Based on the Laplacian obtained from the spectral embedding of the data, it obtains  
105 a score based on locality preservation. SPEC (Zhao and Liu, 2007) is a framework that contains this  
106 previous approach, but it additionally allows for both supervised or unsupervised learning, including  
107 other similarity metrics, as well as other ranking functions. These approaches evaluate each feature  
108 independently, without considering feature interactions. These interactions are, however, taken into  
109 account in Multi-Cluster Feature Selection (MCFS) (Cai et al., 2010), where a multi-cluster approach  
110 is defined based on the eigendecomposition of a similarity matrix. The subset selection is performed  
111 applying an  $l_1$ -norm regularizer to approximate the eigenvectors obtained from the spectral embedding  
112 of the data inducing sparsity. In UDFS (Yang et al., 2011) the  $l_1$ -norm regularizer is substituted by a  
113  $l_{2,1}$ -norm to apply sample and feature-wise constraints, and a discriminative analysis is added in the graph  
114 description. In NDFS (Li et al., 2012), the use of the  $l_{2,1}$ -norm is preserved, but a non-negative constraint  
115 is added to the spectral clustering stage.

116 The aforementioned algorithms perform manifold learning and subset selection in a sequential way.  
117 However, other methods tackle these simultaneously, in order to adaptively change the similarity metric  
118 or the selection criteria regarding the error obtained between the original data and the new representation.  
119 Examples of these algorithms are JELSR (Hou et al., 2013), SOGFS (Nie et al., 2019) and (R)JGSC (Zhu  
120 et al., 2016), and all make use of an  $l_{2,1}$ -norm. Most recently, the SAMM-FS algorithm was proposed  
121 (Zhang et al., 2019), where a combination of similarity measures is used to build the similarity graph,  
122 and the  $l_{2,0}$ -norm is used for regression. This group of algorithms are currently the ones achieving the  
123 best results, at the cost of using complex optimization techniques to adaptively tune both stages of the  
124 feature selection process. While this can lead to good results, it comes with a high computation cost,  
125 which might hamper the tuning process, or might simply not be worthy for some applications. SAMM-FS  
126 and SOGFS are the ones that more specifically suggest new approaches to perform the embedding stage,  
127 by optimally creating the graph (Nie et al., 2019) or deriving it from a combination of different similarity  
128 metrics (Zhang et al., 2019). Again, both approaches require computationally expensive optimization  
129 techniques to select a subset of features.

130 In summary, even if SSFS methods are getting more sophisticated and accurate, this results in  
131 algorithms becoming more complex in terms of computational time, and in the ease of use. The use of  
132 advanced numerical optimization techniques to improve results makes algorithms more complex, and  
133 requires regularization parameters which are not easy to tune. In this work, the combination of a new  
134 approach to estimate the graph connectivity based on the RBF kernel, together with the use of the utility  
135 metric for subset selection, results in an efficient SSFS algorithm, which is easy to use and with lower  
136 complexity than the state-of-the-art.

## 137 METHODS

138 This section describes the proposed U2FS algorithm, which focuses on selecting the relevant features  
139 in an unsupervised way, at a relatively small computational cost. The method is divided in three parts.  
140 Firstly, the suggested manifold learning approach is explained, where an embedding based on binary  
141 weighting and the RBF kernel are used. Then a method to select the kernel parameter of the RBF kernel  
142 is proposed, specially designed for high-dimensional data. Once the manifold learning stage is explained,  
143 the Utility metric is proposed as a new approach for subset selection.

### 144 Manifold learning considering non-linearities

145 Given is a data matrix  $\mathbf{X} \in \mathbb{R}^{N \times d}$ , with  $\mathbf{X} = [\mathbf{x}_1; \mathbf{x}_2; \dots; \mathbf{x}_N]$ ,  $\mathbf{x}_i = [x_i^{(1)}, x_i^{(2)}, \dots, x_i^{(d)}]$ ,  $i = 1, \dots, N$ ,  $N$  the  
146 number of data points, and  $d$  the number of features (i.e., dimensions) in the data. The aim is to learn the  
147 structure hidden in the  $d$ -dimensional data and approximate it with only a subset of the original features.  
148 In this paper, this structure will be identified by means of clustering, where the dataset is assumed to be  
149 characterized by  $c$  clusters.

150 In spectral clustering, the clustering structure of this data can be obtained by studying the eigenvectors  
 151 derived from a Laplacian built from the original data (Von Luxburg (2007), Biggs et al. (1993)). The  
 152 data is represented using a graph  $G = (\mathcal{V}, \mathcal{E})$ .  $\mathcal{V}$  is the set of vertices  $\mathbf{v}_i$ ,  $i = 1, \dots, N$  where  $\mathbf{v}_i = \mathbf{x}_i$ .  
 153  $\mathcal{E} = \{e_{ij}\}$  with  $i = 1, \dots, N$   $j = 1, \dots, N$  is the set of edges between the vertices where  $\{e_{ij}\}$  denotes the  
 154 edge between vertices  $v_i$  and  $v_j$ . The weight of these edges is determined by the entries  $w_{ij} \geq 0$  of a  
 155 similarity matrix  $\mathbf{W}$ . We define the graph as undirected. Therefore, the similarity matrix  $\mathbf{W}$ , is symmetric  
 156 (since  $w_{ij} = w_{ji}$ , with the diagonal set to  $w_{ii} = 0$ ).

157 Typically,  $\mathbf{W}$  is computed after coding the pairwise distances between all  $N$  data points. There are  
 158 several ways of doing this, such as calculating the  $k$ -nearest neighbours (KNN) for each point, or choosing  
 159 the  $\varepsilon$ -neighbors below a certain distance (Belkin and Niyogi, 2002).

160 In this paper, two similarity matrices are adopted inspired by the work in (Cai et al., 2010), namely a  
 161 binary one and one based on an RBF kernel. The binary weighting is based on KNN, being  $w_{ij} = 1$  if and  
 162 only if vertex  $i$  is within the  $K$  closest points to vertex  $j$ . Being a non-parametric approach, the binary  
 163 embedding allows to simply characterize the connectivity of the data.

164 Additionally, the use of the RBF kernel is considered, which is well suited for non-linearities and  
 165 allows to characterize complex and sparse structures (Von Luxburg, 2007). The RBF kernel is defined as  
 166  $K(\mathbf{x}_i, \mathbf{x}_j) = \exp(-\|\mathbf{x}_i - \mathbf{x}_j\|^2 / 2\sigma^2)$ . The selection of the kernel parameter  $\sigma$  is a long-standing challenge  
 167 in machine learning. For instance, in Cai et al. (2010),  $\sigma^2$  is defined as the mean of all the distances  
 168 between the data points. Alternatively, a rule of thumb, uses the sum of the standard deviations of the data  
 169 along each dimension (Varon et al., 2015). However, the estimation of this parameter is highly influenced  
 170 by the amount of features or dimensions in the data, making it less robust to noise and irrelevant features.  
 171 In the next section, a new and better informed method to approximate the kernel parameter is proposed.

172 The graph  $G$ , defined by the similarity matrix  $\mathbf{W}$ , can be partitioned into multiple disjoint sets. Given  
 173 the focus on multi-cluster data of our approach, the  $k$ -Way Normalized Cut ( $NCut$ ) Relaxation is used,  
 174 as proposed in Ng et al. (2002). In order to obtain this partition, the degree matrix  $\mathbf{D}$  of  $\mathbf{W}$  must be  
 175 calculated.  $\mathbf{D}$  is a diagonal matrix for which each element on the diagonal is calculated as  $D_{ii} = \sum_j W_{i,j}$ .  
 176 The normalized Laplacian  $\mathbf{L}$  is then obtained as  $\mathbf{L} = \mathbf{D}^{-1/2} \mathbf{W} \mathbf{D}^{-1/2}$ , as suggested in Von Luxburg (2007).  
 177 The vectors  $\mathbf{y}$  embedding the data in  $\mathbf{L}$  can be extracted from the eigenvalue problem (Chung and Graham,  
 178 1997):

$$\mathbf{L}\mathbf{y} = \lambda\mathbf{y} \quad (1)$$

179 Given the use of a normalized Laplacian for the data embedding, the vectors  $\mathbf{y}$  must be adjusted using  
 180 the degree matrix  $\mathbf{D}$ :

$$\alpha = \mathbf{D}^{1/2} \mathbf{y}, \quad (2)$$

181 which means that  $\alpha$  is the solution of the generalized eigenvalue problem of the pair  $\mathbf{W}$  and  $\mathbf{D}$ . These  
 182 eigenvectors  $\alpha$  are a new representation of the data, that gathers the most relevant information about the  
 183 structures appearing in the high-dimensional space. The  $c$  eigenvectors, corresponding to the  $c$  highest  
 184 eigenvalues (after excluding the largest one), can be used to characterize the data in a lower dimensional  
 185 space (Ng et al., 2002). Thus, the matrix  $\mathbf{E} = [\alpha_1, \alpha_2, \dots, \alpha_c]$  containing column-wise the  $c$  selected  
 186 eigenvectors, will be the low-dimensional representation of the data to be mimicked using a subset of the  
 187 original features, as suggested in Cai et al. (2010).

### 188 Kernel parameter approximation for high-dimensional data

189 One of the most used similarity functions is the RBF kernel, which allows to explore non-linearities in  
 190 the data. Nevertheless, the kernel parameter  $\sigma^2$  must be selected correctly, to avoid overfitting or the  
 191 allocation of all data points to the same cluster. This work proposes a new approach to approximate this  
 192 kernel parameter, which will be denoted by  $\hat{\sigma}^2$  when derived from our method. This method takes into  
 193 account the curse of dimensionality and the potential irrelevant features or dimensions in the data.

194 As a rule of thumb,  $\sigma^2$  is approximated as the sum of the standard deviation of the data along each  
 195 dimension (Varon et al., 2015). This approximation grows with the number of features (i.e. dimensions)  
 196 of the data, and thus, it is not able to capture its underlying structures in high-dimensional spaces.

197 Nevertheless, this  $\sigma^2$  is commonly used as an initialization value, around which a search is performed,  
198 considering some objective function (Alzate and Suykens, 2008; Varon et al., 2015).

199 The MCFS algorithm skips the search around an initialization of the  $\sigma^2$  value by substituting the sum  
200 of the standard deviations by the mean of these (Cai et al., 2010). By doing so, the value of  $\sigma^2$  does not  
201 overly grow. This estimation of  $\sigma^2$  suggested in Cai et al. (2010) will be referred to as  $\sigma_0^2$ . A drawback of  
202 this approximation in high-dimensional spaces is that it treats all dimensions as equally relevant for the  
203 final estimation of  $\sigma_0^2$ , regardless of the amount of information that they actually contain.

204 The aim of the proposed approach is to provide a functional value of  $\sigma^2$  that does not require  
205 any additional search, while being robust to high-dimensional data. Therefore, this work proposes an  
206 approximation technique based on two factors: the distances between the points, and the number of  
207 features or dimensions in the data.

208 The most commonly used distance metric is the euclidean distance. However, it is very sensitive to  
209 high-dimensional data, deriving unsubstantial distances when a high number of features is involved in the  
210 calculation (Aggarwal et al., 2001). In this work, the use of the Manhattan or taxicab distance (Reynolds,  
211 1980) is proposed, given its robustness when applied to high-dimensional data (Aggarwal et al., 2001).  
212 For each feature  $l$ , the Manhattan distance  $\delta_l$  is calculated as:

$$\delta_l = \frac{1}{N} \sum_{i,j=1}^N |x_{il} - x_{jl}| \quad (3)$$

213 Additionally, in order to reduce the impact of irrelevant or redundant features, a system of weights  
214 is added to the approximation of  $\hat{\sigma}^2$ . The goal is to only take into account the distances associated to  
215 features that contain relevant information about the structure of the data. To calculate these weights, the  
216 probability density function (PDF) of each feature is compared with a Gaussian distribution. Higher  
217 weights are assigned to the features with less Gaussian behavior, i.e. those the PDF of which differs the  
218 most from a Gaussian distribution. By doing so, these will influence more the final  $\hat{\sigma}^2$  value, since they  
219 allow a better separation of the structures present in the data.

220 Figure 1 shows a graphical representation of this estimation. The dataset in the example has 3  
221 dimensions or features:  $f_1$ ,  $f_2$  and  $f_3$ .  $f_1$  and  $f_2$  contain the main clustering information, as it can be  
222 observed in Figure 1a, while  $f_3$  is a noisy version of  $f_1$ , derived as  $f_3 = f_1 + 1.5n$ , where  $n$  is drawn from  
223 a normal distribution  $\mathcal{N}(0, 1)$ . Figures 1b, 1c and 1d show in a continuous black line the PDFs derived  
224 from the data, and in a grey dash line their fitted Gaussian, in dimensions  $f_1$ ,  $f_2$  and  $f_3$  respectively. This  
225 fitted Gaussian was derived using the Curve Fitting toolbox of Matlab<sup>TM</sup>. As it can be observed, the  
226 matching of a Gaussian with an irrelevant feature is almost perfect, while those features that contain more  
227 information, like  $f_1$  and  $f_2$ , deviate much more from a normal distribution.

228 Making use of these differences, an error, denoted  $\phi_l$ , for each feature  $l$ , where  $l = 1, \dots, d$ , is  
229 calculated as:

$$\phi_l = \frac{1}{H} \sum_{i=1}^H (p_i - g_i)^2, \quad (4)$$

230 where  $H$  is the number of bins in which the range of the data is divided to estimate the PDF ( $p$ ), and  $g$   
231 is the fitted Gaussian. The number of bins in this work is set to 100 for standardization purposes. Equation  
232 (4) corresponds to the mean-squared error (MSE) between the PDF of the data over feature  $l$  and its fitted  
233 Gaussian. From these  $\phi_l$ , the final weights  $b_l$  are calculated as:

$$b_l = \frac{\phi_l}{\sum_{l=1}^d \phi_l} \quad (5)$$

234 Therefore, combining (3) and (5), the proposed approximation, denoted  $\hat{\sigma}^2$ , is derived as:

$$\hat{\sigma}^2 = \sum_{l=1}^d b_l \delta_l, \quad (6)$$

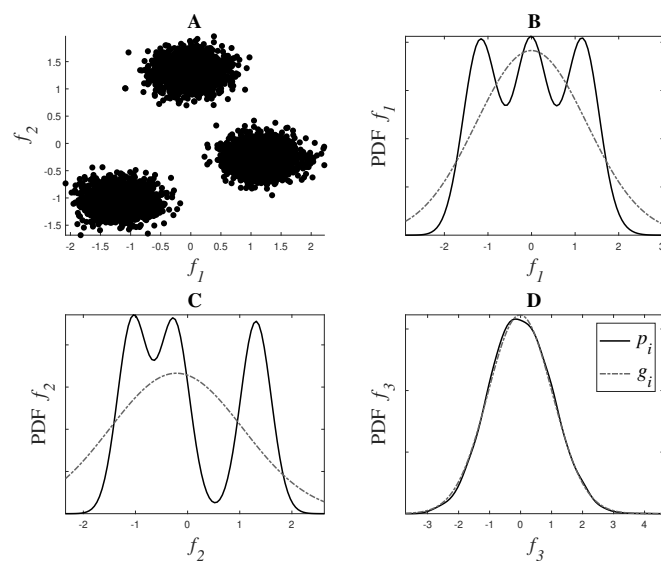


**Figure 1.** Weight system for relevance estimation. In Figure 1A,  $f_1$  and  $f_2$  can be seen. 1B, 1C and 1D show in black the PDFs  $p_i$  of  $f_1$ ,  $f_2$  and  $f_3$  respectively, and in grey dotted line their fitted Gaussian  $g_i$ .

235 which gathers the distances present in the most relevant features, giving less importance to the  
 236 dimensions that do not contribute to describe the structure of the data. The complete algorithm to calculate  
 237  $\hat{\sigma}^2$  is described in Algorithm 1.

---

**Algorithm 1** Kernel parameter approximation for high-dimensional data.

---

**Input:** Data  $\mathbf{X} \in \mathbb{R}^{N \times d}$ .

**Output:** Sigma parameter  $\hat{\sigma}^2$

- 1: Calculate the Manhattan distances between the datapoints using Equation (3): vector of distances per feature  $\delta_i$ .
  - 2: Obtain the weights for each of the features using Equations (4) and (5): weights  $b_i$ .
  - 3: Calculate  $\hat{\sigma}^2$  using Equation (6).
- 

### 238 Utility metric for feature subset selection

239 In the manifold learning stage, a new representation  $\mathbf{E}$  of the data based on the eigenvectors was built,  
 240 which described the main structures present in the original high-dimensional data. The goal is to select  
 241 a subset of the features which best approximates the data in this new representation. In the literature,  
 242 this feature selection problem is formulated using a graph-based loss function and a sparse regularizer  
 243 of the coefficients is used to select a subset of features, as explained in Zhu et al. (2016). The main  
 244 idea of these approaches is to regress the data to its low dimensional embedding along with some sparse  
 245 regularization. The use of such regularization techniques reduces overfitting and achieves dimensionality  
 246 reduction. This regression is generally formulated as a least squares (LS) problem, and in many of these  
 247 cases, the metric that is used for feature selection is the magnitude of their corresponding weights in  
 248 the least squares solution (Cai et al., 2010; Gui et al., 2016). However, the optimized weights do not  
 249 necessarily reflect the importance of the corresponding feature as it is scaling dependent and it does  
 250 not properly take interactions across features into account (Bertrand, 2018). Instead, the importance  
 251 of a feature can be quantified using the increase in least-squared error (LSE) if that feature was to be  
 252 removed and the weights were re-optimized. This increase in LSE, called the ‘utility’ of the feature can  
 253 be efficiently computed (Bertrand, 2018) and can be used as an informative metric for a greedy backwards  
 254 feature selection procedure (Bertrand, 2018; Narayanan and Bertrand, 2020; Szurley et al., 2014), as an  
 255 alternative for (group-)LASSO based techniques. Under some technical conditions, a greedy selection  
 256 based on this utility metric can even be shown to lead to the optimal subset (Couvreur and Bresler, 2000).

After representing the dataset using the matrix  $\mathbf{E} \in \mathbb{R}^{N \times c}$  containing the  $c$  eigenvectors, the following

LS optimization problem finds the weights  $\mathbf{p}$  that best approximate the data  $\mathbf{X}$  in the  $c$ -dimensional representation in  $\mathbf{E}$ :

$$J = \min_{\mathbf{p}} \frac{1}{N} \|\mathbf{X}\mathbf{p} - \mathbf{E}\|_F^2 \quad (7)$$

257 where  $J$  is the cost or the LSE and  $\|\cdot\|_F$  denotes the Frobenius norm.

If  $\mathbf{X}$  is a full rank matrix and if  $N > d$ , the LS solution  $\hat{\mathbf{p}}$  of (7) is

$$\hat{\mathbf{p}} = \mathbf{R}_{\mathbf{X}\mathbf{X}}^{-1} \mathbf{R}_{\mathbf{X}\mathbf{E}}, \quad (8)$$

258 with  $\mathbf{R}_{\mathbf{X}\mathbf{X}} = \frac{1}{N} \mathbf{X}^T \mathbf{X}$  and  $\mathbf{R}_{\mathbf{X}\mathbf{E}} = \frac{1}{N} \mathbf{X}^T \mathbf{E}$ .

259 The goal of this feature selection method is to select the subset of  $s (< d)$  features that best represents  
260  $\mathbf{E}$ . This feature selection problem can be reduced to the selection of the best  $s (< d)$  columns of  $\mathbf{X}$  which  
261 minimize (7). However, this is inherently a combinatorial problem and is computationally unfeasible to  
262 solve. Nevertheless, several greedy and approximative methods have been proposed (Gui et al., 2016; Nie  
263 et al., 2019; Narayanan and Bertrand, 2020). In the current work, the use of the utility metric for subset  
264 selection is proposed to select these best  $s$  columns.

265 The utility of a feature  $l$  of  $\mathbf{X}$ , in an LS problem like (7), is defined as the increase in the LSE  $J$  when  
266 the column corresponding to the  $l$ -th feature in  $\mathbf{X}$  is removed from the problem and the new optimal  
267 weight matrix,  $\hat{\mathbf{p}}_{-l}$ , is re-computed similar to (8). Consider the new LSE after the removal of feature  $l$   
268 and the re-computation of the weight matrix  $\hat{\mathbf{p}}_{-l}$  to be  $J_{-l}$ , defined as:

$$J_{-l} = \frac{1}{N} \|\mathbf{X}_{-l} \hat{\mathbf{p}}_{-l} - \mathbf{E}\|_F^2 \quad (9)$$

269 where  $\mathbf{X}_{-l}$  denotes the matrix  $\mathbf{X}$  with the column corresponding to  $l$ -th feature removed. Then  
270 according to the definition, the utility of feature  $l$ ,  $U_l$  is:

$$U_l = J_{-l} - J \quad (10)$$

271 A straightforward computation of  $U_l$  would be computationally heavy due to the fact that the compu-  
272 tation of  $\hat{\mathbf{p}}_{-l}$  requires a matrix inversion of  $\mathbf{X}_{-l} \mathbf{X}_{-l}^T$ , which has to be repeated for each feature  $l$ .

273 However, it can be shown that the utility of the  $l$ -th feature of  $\mathbf{X}$  in (10) can be computed efficiently  
274 without the explicit recomputation of  $\hat{\mathbf{p}}_{-l}$  by using the following expression (Bertrand, 2018):

$$U_l = \frac{1}{q_l} \|\bar{\mathbf{p}}_l\|_2, \quad (11)$$

275 where  $q_l$  is the  $l$ -th diagonal element of  $\mathbf{R}_{\mathbf{X}\mathbf{X}}^{-1}$  and  $p_l$  is the  $l$ -th row in  $\hat{\mathbf{p}}$ , corresponding to the  $l$ -th  
276 feature. The mathematical proof of (11) can be found in Bertrand (2018). Note that  $\mathbf{R}_{\mathbf{X}\mathbf{X}}^{-1}$  is already known  
277 from the computation of  $\hat{\mathbf{p}}$  such that no additional matrix inversion is required.

278 However, since the data matrix  $\mathbf{X}$  can contain redundant features or features that are linear combi-  
279 nations of each other in its columns, it cannot be guaranteed that the matrix  $\mathbf{X}$  in (7) is full-rank. In  
280 this case, the removal of a redundant column from  $\mathbf{X}$  will not lead to an increase in the LS cost of (7).  
281 Moreover,  $\mathbf{R}_{\mathbf{X}\mathbf{X}}^{-1}$ , used to find the solution of (7) in (8), will not exist in this case since the matrix  $\mathbf{X}$  is rank  
282 deficient. A similar problem appears if  $N < d$ , which can happen in case of very high-dimensional data.  
283 To overcome this problem, the definition of utility generalized to a minimum  $l_2$ -norm selection (Bertrand,  
284 2018) is used in this work. This approach eliminates the feature yielding the smallest increase in the  
285  $l_2$ -norm of the weight matrix when the column corresponding to that feature were to be removed and the  
286 weight matrix would be re-optimized. Moreover, minimizing the  $l_2$ -norm of the weights further reduces  
287 the risk of overfitting.

288 This generalization is achieved by first adding an  $l_2$ -norm penalty  $\beta$  to the cost function that is  
289 minimized in (7):

$$J = \min_{\mathbf{p}} \frac{1}{2} \|\mathbf{X}\mathbf{p} - \mathbf{E}\|_F^2 + \beta \|\mathbf{p}\|_2^2 \quad (12)$$

290 where  $0 < \beta \leq \mu$  with  $\mu$  equal to the smallest non-zero eigenvalue of  $\mathbf{R}_{\mathbf{X}\mathbf{X}}$  in order to ensure that the  
 291 bias added due to the penalty term in (12) is negligible. The minimizer of (12) is:

$$\hat{\mathbf{p}} = \mathbf{R}_{\mathbf{X}\mathbf{X}\beta}^{-1} \mathbf{R}_{\mathbf{X}\mathbf{E}} = (\mathbf{R}_{\mathbf{X}\mathbf{X}} + \beta \mathbf{I})^{-1} \mathbf{R}_{\mathbf{X}\mathbf{E}} \quad (13)$$

292 It is noted that (13) reduces to  $\mathbf{R}_{\mathbf{X}\mathbf{X}}^{\dagger} \mathbf{R}_{\mathbf{X}\mathbf{E}}$  when  $\beta \rightarrow 0$ , where  $\mathbf{R}_{\mathbf{X}\mathbf{X}}^{\dagger}$  denotes the Moore-Penrose pseudo-  
 293 inverse. This solution corresponds to the minimum norm solution of (7) when  $\mathbf{X}$  contains linearly  
 294 dependent columns or rows. The utility  $U_l$  of the  $l$ -th column in  $\mathbf{X}$  based on (12) is (Bertrand, 2018):

$$\begin{aligned} U_l &= (\|\mathbf{X}_{-l} \hat{\mathbf{p}}_{-l} - \mathbf{E}\|_2^2 - \|\mathbf{X} \hat{\mathbf{p}} - \mathbf{E}\|_2^2) \\ &\quad + \beta (\|\hat{\mathbf{p}}_{-l}\|_2^2 - \|\hat{\mathbf{p}}\|_2^2) \\ &= (J_{-l} - J) + \beta (\|\hat{\mathbf{p}}_{-l}\|_2^2 - \|\hat{\mathbf{p}}\|_2^2) \end{aligned} \quad (14)$$

295 Note that if column  $l$  in  $\mathbf{X}$  is linearly independent from the other columns, (14) closely approximates  
 296 to the original utility definition in (10) as the first term dominates over the second. However, if column  $l$   
 297 is linearly dependent, the first term vanishes and the second term will dominate. In this case, the utility  
 298 quantifies the increase in  $l_2$ -norm after removing the  $l$ -th feature.

299 To select the best  $s$  features of  $\mathbf{X}$ , a greedy selection based on the iterative elimination of the features  
 300 with the least utility is carried out. After the elimination of each feature, a re-estimation of the weights  $\hat{\mathbf{p}}$   
 301 is carried out and the process of elimination is repeated, until  $s$  features remain.

302 Note that the value of  $\beta$  depends on the smallest non-zero eigenvalue of  $\mathbf{R}_{\mathbf{X}\mathbf{X}}$ . Since  $\mathbf{R}_{\mathbf{X}\mathbf{X}}$  has to be  
 303 recomputed every time when a feature is removed, also its eigenvalues change along the way. In practice,  
 304 the value of  $\beta$  is selected only once and fixed for the remainder of the algorithm, as smaller than the  
 305 smallest non-zero eigenvalue of  $\mathbf{R}_{\mathbf{X}\mathbf{X}}$  before any of the features are eliminated (Narayanan and Bertrand,  
 306 2020). This value of  $\beta$  will be smaller than all the non-zero eigenvalues of any principal submatrix of  
 307  $\mathbf{R}_{\mathbf{X}\mathbf{X}}$  using the Cauchy's interlace theorem (Hwang, 2004).

308 The summary of the utility subset selection is described in Algorithm 2. Algorithm 3 outlines the  
 309 complete U2FS algorithm proposed in this paper.

---

**Algorithm 2** Utility metric algorithm for subset selection.

---

**Input:** Data  $\mathbf{X}$ , Eigenvectors  $\mathbf{E}$ , Number of features  $s$  to select

**Output:**  $s$  features selected

- 1: Calculate  $\mathbf{R}_{\mathbf{X}\mathbf{X}}$  and  $\mathbf{R}_{\mathbf{X}\mathbf{E}}$  as described in Equation (8).
  - 2: Calculate  $\beta$  as the smallest non-zero eigenvalue of  $\mathbf{R}_{\mathbf{X}\mathbf{X}}$
  - 3: **while** Number of features remaining is  $> s$  **do**
  - 4:   Compute  $\mathbf{R}_{\mathbf{X}\mathbf{X}\beta}^{-1}$  and  $\hat{\mathbf{p}}$  as described in (13).
  - 5:   Calculate the utility of the remaining features using (11)
  - 6:   Remove the feature  $f_l$  with the lowest utility.
  - 7:   Update  $\mathbf{R}_{\mathbf{X}\mathbf{X}}$  and  $\mathbf{R}_{\mathbf{X}\mathbf{E}}$  by removing the rows and columns related to that feature  $f_l$ .
  - 8: **end while**
- 

---

**Algorithm 3** Unsupervised feature selector based on the utility metric (U2FS).

---

**Input:** Data  $\mathbf{X}$ , Number of clusters  $c$ , Number of features  $s$  to select

**Output:**  $s$  features selected

- 1: Construct the similarity graph  $\mathbf{W}$  as described in Section selecting one of the weightings:
    - Binary
    - RBF kernel, using  $\sigma_0^2$
    - RBF kernel, using  $\hat{\sigma}^2$  based on Algorithm 1
  - 2: Calculate the normalized Laplacian  $\mathbf{L}$  and the eigenvectors  $\alpha$  derived from Equation (2).  
 Keep the  $c$  eigenvectors corresponding to the highest eigenvalues, excluding the first one.
  - 3: Apply the backward greedy utility algorithm 2.
  - 4: Return the  $s$  features remaining from the backward greedy utility approach.
-

310 As it has been stated before, one of the most remarkable aspects of the U2FS algorithm is the use of  
 311 a greedy technique to solve the subset selection problem. The use of this type of method reduces the  
 312 computational cost of the algorithm. This can be confirmed analyzing the computational complexity of  
 313 U2FS, where the most demanding steps are the eigendecomposition of the Laplacian matrix (step 2 of  
 314 Algorithm 3), which has a cost of  $O(N^3)$  (Tsironis et al., 2013), and the subset selection stage in step 3 of  
 315 Algorithm 3. Contrary to the state-of-the-art, the complexity of U2FS being a greedy method depends on  
 316 the number of features to select. The most computationally expensive step of the subset selection in U2FS  
 317 is the calculation of the matrix  $\mathbf{R}_{\mathbf{X}\mathbf{X}}^{-1}$ , which has a computational cost of  $O(d^3)$ . In addition, this matrix  
 318 needs to be updated  $d - s$  times. This update can be done efficiently using a recursive updating equation  
 319 from Bertrand (2018) with a cost of  $O(t^2)$ , with  $t$  the number of features remaining in the dataset, i.e.  
 320  $t = d - s$ . Since  $t < d$ , the cost for performing  $d - s$  iterations will be  $O((d - s)d^2)$ , which depends on  
 321 the number of features  $s$  to be selected. Note that the cost of computing the least squares solution  $\hat{\mathbf{p}}_{-l}$  for  
 322 each  $l$  in (14) is eliminated using the efficient equation (11), bringing down the cost for computing the  
 323 utility from  $O(t^4)$  to  $O(t)$  in each iteration. This vanishes with respect to the  $O(d^3)$  term (remember that  
 324  $t < d$ ). Therefore, the total asymptotic complexity of U2FS is  $O(N^3 + d^3)$ .

## 325 RESULTS

326 The aim of the following experiments is to evaluate the U2FS algorithm based on multiple criteria. With  
 327 the focus on the new estimation of the embedding proposed, the proposed RBF kernel approach using  
 328 the estimated  $\hat{\sigma}^2$  is compared to the  $\sigma_0^2$  parameter proposed in Cai et al. (2010), and to the binary KNN  
 329 graph commonly used in Gui et al. (2016). On the other hand, the utility metric for subset selection is  
 330 compared to other sparsity-inducing techniques, based on  $l_p$ -norm regularizations. In these experiments,  
 331 this is evaluated using the  $l_1$ -norm. The outline of the different combinations considered in this work  
 332 summarized in Table 1. The last method, RBF $_{\hat{\sigma}^2}$  + Utility, would be the one referred to as U2FS,  
 333 combining the novelties suggested in this work.

**Table 1.** Methods compared in the experiments

	Similarity measure	Subset selection
<b>KNN<math>_{Bin}</math> + <math>l_1</math> - norm</b>	KNN + binary weighting	$l_1$ -norm
<b>RBF<math>_{\sigma_0^2}</math> + <math>l_1</math> - norm</b>	RBF kernel, $\sigma_0^2$	$l_1$ -norm
<b>KNN<math>_{Bin}</math> + Utility</b>	KNN + binary weighting	Utility metric
<b>RBF<math>_{\sigma_0^2}</math> + Utility</b>	RBF kernel, $\sigma_0^2$	Utility metric
<b>RBF<math>_{\hat{\sigma}^2}</math> + Utility</b>	RBF kernel, $\hat{\sigma}^2$	Utility metric

334 These novelties are evaluated in two different scenarios, namely a simulation study, and in the  
 335 application of the methods on benchmark datasets. In particular for the latter, the methods are not only  
 336 evaluated in terms of accuracy, but also regarding computational complexity. These evaluations are  
 337 performed against the state-of-the-art.

## 338 Simulations

339 A set of nonlinear toy examples typically used in clustering problems are proposed to test the different  
 340 feature selection methods. In these experiments, the goal was to verify the correct selection of the original  
 341 set of features. Figure 2 shows the toy examples considered<sup>2</sup>, which are described by features  $f_1$  and  $f_2$ ,  
 342 and the final description of the datasets can be seen in Table 2.

343 All these problems are balanced, except for the last dataset Cres-Moon, for which the data is divided  
 344 25% to 75% between the two clusters. Five extra features in addition to the original  $f_1$  and  $f_2$  were added  
 345 to each of the datasets in order to include redundant or irrelevant information:

- 346 •  $f'_1$  and  $f'_2$ : random values extracted from two Pearson distributions characterized by the same  
 347 higher-order statistics as  $f_1$  and  $f_2$  respectively.
- 348 •  $f'_3$  and  $f'_4$ : Original  $f_1$  and  $f_2$  contaminated with Gaussian noise ( $v\mathcal{N}(0, 1)$ ), with  $v = 1.5$ .
- 349 •  $f'_5$ : Constant feature of value 0.

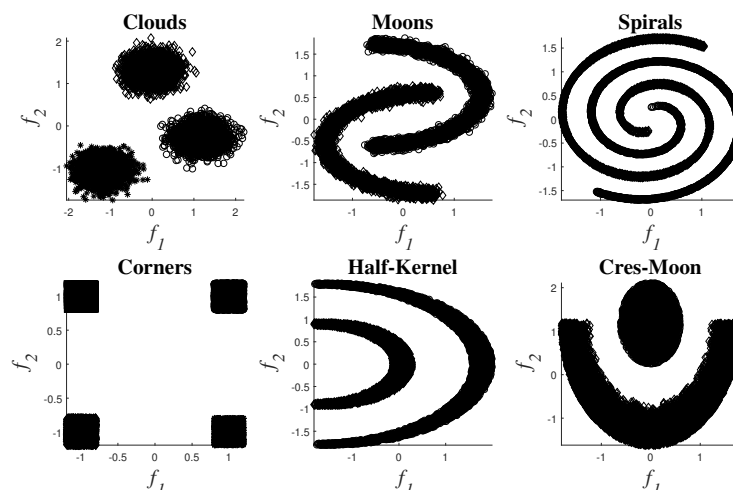


**Figure 2.** Toy examples used for simulations.

**Table 2.** Description of the toy example datasets.

	# samples	# classes
<b>Clouds</b>	9000	3
<b>Moons</b>	10000	2
<b>Spirals</b>	10000	2
<b>Corners</b>	10000	4
<b>Half-Kernel</b>	10000	2
<b>Crescent-Moon</b>	10000	2

350 The first step in the preprocessing of the features was to standardize the data using z-score to reduce  
 351 the impact of differences in scaling and noise. In order to confirm the robustness of the feature selection  
 352 techniques, the methods were applied using 10-fold cross-validation on the standardized data. For each  
 353 fold a training set was selected using  $m$ -medoids, setting  $m$  to 2000 and using the centers of the clusters  
 354 found as training samples. By doing so, the generalization ability of the methods can be guaranteed  
 355 (Varon et al., 2015). On each of the 10 training sets, the features were selected applying the 5 methods  
 356 mentioned in Table 1. For each of the methods, the number of clusters  $c$  was introduced as the number of  
 357 classes presented in Table 2. Since these experiments aim to evaluate the correct selection of the features,  
 358 and the original features  $f_1$  and  $f_2$  are known, the number of features  $s$  to be selected was set to 2.

359 Regarding the parameter settings within the embedding methods, the binary was obtained setting  $k$  in  
 360 the  $k$ NN approach to 5. For the RBF kernel embedding,  $\sigma_0^2$  was set to the mean of the standard deviation  
 361 along each dimension, as done in Cai et al. (2010). When using  $\hat{\sigma}^2$ , its value was obtained by applying  
 362 the method described in Algorithm 1.

363 In terms of subset selection approaches, the method based on the  $l_1$ -norm automatically sets the  
 364 value of the regularization parameter required for the LARS implementation, as described in (Deng Cai,  
 365 Chiyuan Zhang, 2020). For the utility metric,  $\beta$  was automatically set to the smallest non-zero eigenvalue  
 366 of the matrix  $\mathbf{R}_{XX}$  as described in Algorithm 2.

367 The performance of the algorithm is evaluated comparing the original set of features  $f_1$  and  $f_2$  to those  
 368 selected by the algorithm. In these experiments, the evaluation of the selection results is binary: either the  
 369 feature set selected is correct or not, regardless of the additional features  $f'_i$ , for  $i = 1, 2, \dots, 5$ , selected.

370 In Table 3 the most common results obtained in the 10 folds are shown. The utility-based approaches  
 371 always obtained the same results for all 10 folds of the experiments. On the contrary, the  $l_1$ -norm  
 372 methods provided different results for different folds of the experiment. For these cases, Table 3 shows  
 373 the most common feature pair for each experiment, occurring at least 3 times.

<sup>2</sup>The codes used to generate these datasets are available in <https://github.com/avillago/u2fs>

**Table 3.** Results feature selection for toy examples

Method	Utility metric			$l_1 - norm$	
	$KNN_{Bin}$	$RBF_{\sigma_0^2}$	$RBF_{\hat{\sigma}^2}$	$KNN_{Bin}$	$RBF_{\sigma_0^2}$
<b>Clouds</b>	$f_1, f_2$	$f'_1, f'_4$	$f_1, f_2$	$f'_1, f'_2$	$f'_1, f'_2$
<b>Moons</b>	$f_1, f_2$	$f'_3, f'_4$	$f_1, f_2$	$f'_1, f'_3$	$f'_1, f'_3$
<b>Spirals</b>	$f_1, f_2$	$f_1, f_2$	$f_1, f_2$	$f_2, f'_2$	$f_2, f'_2$
<b>Corners</b>	$f_1, f_2$	$f'_1, f'_2$	$f_1, f_2$	$f_2, f'_2$	$f_2, f'_2$
<b>Half-Kernel</b>	$f_1, f_2$	$f_2, f'_3$	$f_1, f_2$	$f_1, f'_3$	$f_1, f'_3$
<b>Cres-Moon</b>	$f_1, f_2$	$f_1, f'_4$	$f_1, f_2$	$f_2, f'_1$	$f_2, f'_2$

374 As shown in Table 3, the methods that always obtain the adequate set of features are based on utility,  
 375 both with the binary weighting and with the RBF kernel and the suggested  $\hat{\sigma}^2$ . Since these results were  
 376 obtained for the 10 folds, they confirm both the robustness and the consistency of the U2FS algorithm.

### 377 Benchmark datasets

378 Additionally, the proposed methods were evaluated using 6 well-known benchmark databases. The  
 379 databases considered represent image (USPS, ORL, COIL20), audio (ISOLET) and text data (PCMAC,  
 380 BASEHOCK)<sup>3</sup>, proposing examples with more samples than features, and vice versa. The description of  
 381 these databases is detailed in Table 4.

**Table 4.** Description of the benchmark databases

	Data Type	Samples	Features	Classes
<b>USPS</b>	Images	9298	256	10
<b>Isolet</b>	Audio	1560	617	26
<b>ORL</b>	Images	400	1024	40
<b>COIL20</b>	Images	1440	1024	20
<b>PCMAC</b>	Text	1943	3289	2
<b>BASEHOCK</b>	Text	1993	4862	2

382 In these datasets, the relevant features are unknown. Therefore, the common practice in the literature  
 383 to evaluate feature selectors consists of applying the algorithms, taking from 10 to 80% of the original  
 384 set of features, and evaluating the accuracy of a classifier when trained and evaluated with the selected  
 385 feature set (Zhu et al., 2016). The classifier used for this aim in other papers is  $k$ -Nearest Neighbors  
 386 (KNN), setting the number of neighbors to 5.

387 These accuracy results are computed using 10-fold cross-validation to confirm the generalization  
 388 capabilities of the algorithm. By setting  $m$  to 90% of the number of samples available in each benchmark  
 389 dataset,  $m$ -medoids is used to select the  $m$  centroids of the clusters and use them as training set. Feature  
 390 selection and the training of the KNN classifier are performed in these 9 folds of the standardized data,  
 391 and the accuracy of the KNN is evaluated in the remaining 10% for testing. Exclusively for USPS, given  
 392 the size of the dataset, 2000 samples were used for training and the remaining data was used for testing.  
 393 These 2000 samples were also selected using  $m$ -medoids. Since PCMAC and BASEHOCK consist of  
 394 binary data, these datasets were not standardized.

395 The parameters required for the binary and RBF embeddings, as well as  $\beta$  for the utility algorithm,  
 396 are automatically set as detailed in section .

397 Figure 3 shows the median accuracy obtained for each of the 5 methods. The shadows along the  
 398 lines correspond to the 25 and 75 percentile of the 10 folds. As a reference, the accuracy of the classifier  
 399 without using feature selection is shown in black for each of the datasets. Additionally, Figure 4 shows the  
 400 computation time for both the utility metric and the  $l_1 - norm$  applied on a binary weighting embedding.  
 401 In this manner, the subset selection techniques can be evaluated regardless of the code efficiency of the  
 402 embedding stage. Similarly to Figure 3, the computation time plots show in bold the median running time

<sup>3</sup>All datasets downloaded from <http://featureselection.asu.edu/datasets.php>

403 for each of the subset selection techniques, and the 25 and 75 percentiles around it obtained from the  
404 10-fold cross-validation.

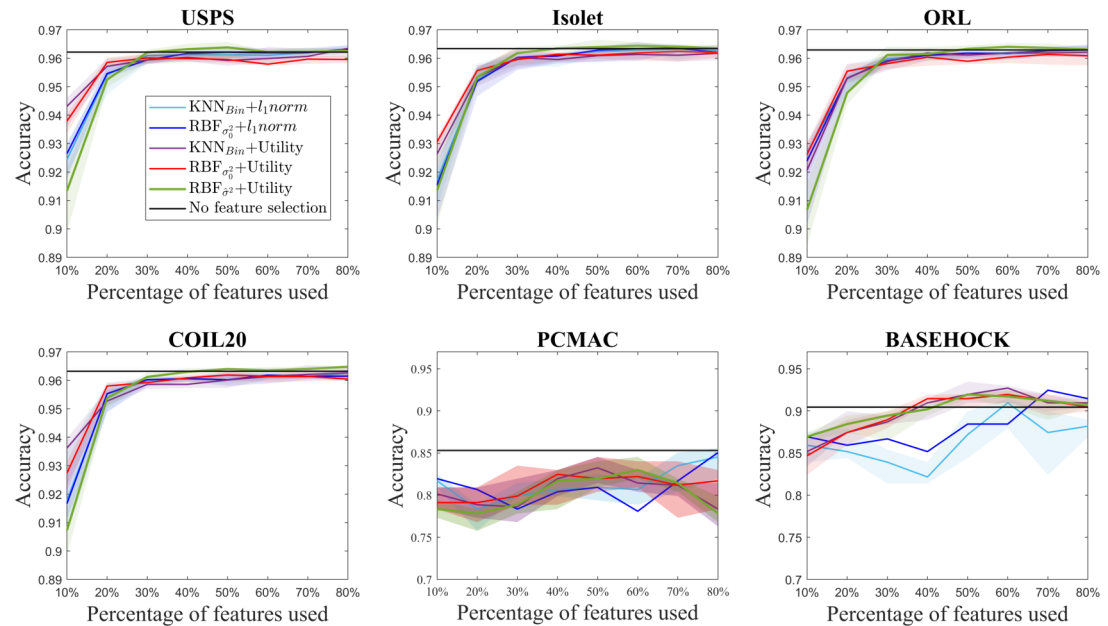


**Figure 3.** Accuracy results for the benchmark databases, for selecting from 10 to 80% of the original number of features. The thick lines represent the median accuracy of the 10-fold cross-validation, and the shadows, the 25 and 75 percentile.

405 The difference in the trends of the  $l_1 - norm$  and utility in terms of computation time is due to their  
406 formulation. Feature selection based on  $l_1 - norm$  regularization, solved using the LARS algorithm in  
407 this case, requires the same computation time regardless of the number of features aimed to select. All  
408 features are evaluated together, and later on, an MCFS score obtained from the regression problem is  
409 assigned to them (Cai et al., 2010). The features with the higher scores are the ones selected. On the other  
410 hand, since the utility metric is applied in a backward greedy trend, the computation times change for  
411 different number of features selected. The lower the number of features selected compared to the original  
412 set, the higher the computation time. This is aligned with the computational complexity of the algorithm,  
413 described in Section . In spite of this, it can be seen that even the highest computation time for utility is  
414 lower than the time taken using  $l_1 - norm$  regularization. The experiments were performed with 2x Intel  
415 Xeon E5-2640 @ 2.5 GHz processors and 64GB of working memory.

416 Additionally, in order to compare the results of U2FS with more methods from the state-of-the-art, the  
417 results described in Zhu et al. (2016) for the BASEHOCK and PCMAC datasets are taken as a reference.  
418 The experiment set-up is equivalent to the one previously described, applying KNN to the data after  
419 having selected a subset of the features. Since the method proposed by Zhu et al., RJGSC, achieves the  
420 best results from the state-of-the-art, it is taken as benchmark in this paper. Table 5 summarizes those  
421 results by showing the KNN accuracy (ACC) for 10% of the features used, and the maximum ACC  
422 achieved among the percentages of features considered, for the BASEHOCK and PCMAC datasets. The  
423 algorithms compared are RJGSC, MCFS and U2FS. MCFS can be seen as a simplified version of U2FS,  
424 where the embedding is done using KNN and binary weighting, and the  $l_1 - norm$  is used for subset  
425 selection. U2FS, on the other hand, results from the combination of the RBF kernel with  $\hat{\sigma}^2$  and the utility  
426 metric.

427

## 428 DISCUSSION

429 The results obtained in the experiments suggest that the proposed U2FS algorithm obtains comparable  
430 results to the state-of-the-art in all the applications suggested, taking less computational time. Nevertheless,

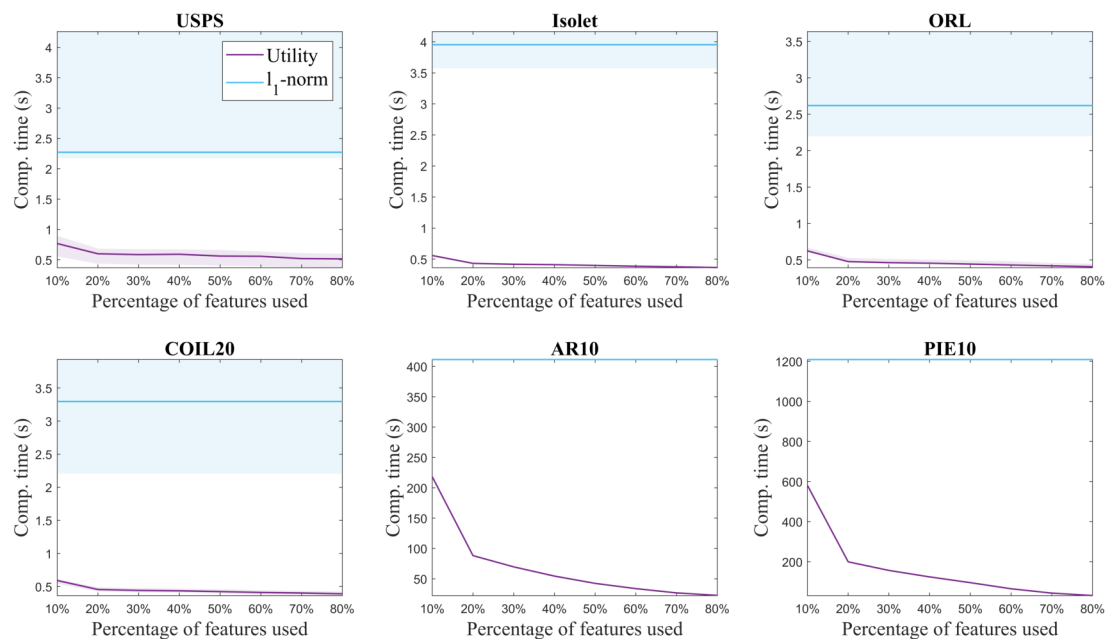


**Figure 4.** Computation time for extracting from 10 to 80% of the original number of features for each of the benchmark databases.

**Table 5.** Comparison of classification accuracy (ACC) with the state-of-the-art for PCMAC and BASEHOCK datasets.

Dataset	Method	ACC at 10% features	% features at Max ACC	Max ACC
PCMAC	<b>U2FS</b>	<b>0.79</b>	<b>60%</b>	<b>0.83</b>
	RJGSC	0.81	60%	0.83
	MCFS	0.67	20%	0.70
BASEHOCK	<b>U2FS</b>	<b>0.87</b>	<b>50%</b>	<b>0.93</b>
	RJGSC	0.90	80%	0.92
	MCFS	0.82	80%	0.84

431 the performance of the utility metric for feature selection varies for the different experiments presented  
432 and requires a detailed analysis.

433 From Table 3, in Section , it can be concluded that the utility metric is able to select the correct  
434 features in an artificially contaminated dataset. Both the binary embedding and the RBF kernel with  $\hat{\sigma}^2$   
435 select the original set of features for the 10 folds of the experiment. The stability in the results also applies  
436 for the RBF embedding with  $\sigma_0^2$ , which always selected the same feature pair for all 10 folds even though  
437 they are only correct for the spirals problem.

438 Therefore, considering the stability of the results, it can be concluded that the proposed approach is  
439 more robust in the selection of results than that based on the  $l_1 - norm$ .

440 On the other hand, when considering the suitability of the features selected, two observations can be  
441 made. First of all, it can be seen that the lack of consistency in the  $l_1 - norm$  approaches discards the  
442 selection of the correct set of features. Moreover, the wrong results obtained with both  $l_1 - norm$  and  
443 utility methods for the RBF embedding using  $\sigma_0^2$  reveal the drawback of applying this approximation  
444 of  $\sigma_0^2$  in presence of redundant or irrelevant features. Since this value is calculated as the mean of the  
445 standard deviation of all the dimensions in the data, this measure can be strongly affected by irrelevant  
446 data, that could be very noisy and enlarge this sigma, leading to the allocation of all the samples to a  
447 mega-cluster.

448 While the use of the proposed approximation for  $\hat{\sigma}^2$  achieves better results than  $\sigma_0^2$ , these are  
449 comparable to the ones obtained with the KNN binary embedding when using the utility metric. The use  
450 of KNN to build graphs is a well-known practice, very robust for dense clusters, as it is the case in these  
451 examples. The definition of a specific field where each of the embeddings would be superior is beyond  
452 the scope of this paper. However, the excellence of both methods when combined with the proposed  
453 subset selection method only confirms the robustness of the utility metric, irrespective of the embedding  
454 considered.

455 For standardization purposes, the performance of the method was evaluated in benchmark databases.  
456 As it can be observed, in terms of the accuracy obtained for each experiment, U2FS achieves comparable  
457 results to the  $l_1 - norm$  methods for most of the datasets considered, despite its condition of greedy  
458 method.

459 In spite of this, some differences in performance can be observed in the different datasets. The different  
460 ranking of the methods, as well as the accuracy obtained for each of the databases can be explained taking  
461 into account the type of data under study and the ratio between samples and dimensions.

462 With regard to the type of data represented by each test, it can be observed that for the ISOLET dataset,  
463 containing sound information, two groups of results are distinguishable. The group of the utility metric  
464 results outperforms those derived from the  $l_1 - norm$ , which only reach comparable results for 60% of the  
465 features selected. These two groups of results are caused by the subset selection method applied, and not  
466 for the embedding, among which the differences are not remarkable.

467 In a similar way, for the case of the image datasets USPS, ORL and COIL20, the results derived  
468 from utility are slightly better than those coming from the  $l_1 - norm$ . In these datasets, similarly to the  
469 performance observed in ISOLET, accuracy increases with the number of features selected.

470 Regarding the differences between the proposed embeddings, it can be observed that the results  
471 obtained are comparable for all of them. Nonetheless, Figure 3 shows that there is a slight improvement  
472 in the aforementioned datasets for the RBF kernel with  $\hat{\sigma}^2$ , but the results are still comparable to those  
473 obtained with other embeddings. Moreover, this similarity in the binary and RBF results holds for the  
474  $l_1 - norm$  methods, for which the accuracy results almost overlap in Figure 3. This can be explained by  
475 the relation between the features considered. Since for these datasets the samples correspond to pixels,  
476 and the features to the color codes, a simple neighboring method such as the binary weighting is able to  
477 code the connectivity of pixels of similar colors.

478 The text datasets, PCMAC and BASEHOCK, are the ones that show bigger differences between the  
479 results obtained with utility and those obtained with the  $l_1 - norm$ . This can be explained by the amount  
480 of zeros present in the data, with which the utility metric is able to cope slightly better. The sparsity of the  
481 data leads to more error in the  $l_1 - norm$  results, since more features end up having the same MCFS score,  
482 and among those, the order for selection comes at random. The results obtained with the utility metric  
483 are more stable, in particular for the BASEHOCK dataset. For this dataset, U2FS even outperforms the  
484 results without feature selection if at least 40% of the features are kept.

485 In all the datasets proposed, the results obtained with the  $l_1 - norm$  show greater variability, i.e. larger

486 percentiles. This is aligned with the results obtained in the simulations. The results for the  $l_1$  – norm  
487 are not necessarily reproducible in different runs, since the algorithm is too sensitive to the training set  
488 selected. The variability of the utility methods is greater for the approaches based on the RBF kernel.  
489 This is due to the selection of the  $\sigma^2$  parameter, which also depends on the training set. The tuning of this  
490 parameter is still very sensitive to high-dimensional and large-scale data, posing a continuous challenge  
491 for the machine learning community (Yin and Yin, 2016; Tharwat et al., 2017).

492 Despite it being a greedy method, the utility metric proves to be applicable to feature selection  
493 approaches and to strongly outperform the  $l_1$  – norm in terms of computational time, without significant  
494 reduction in accuracy. U2FS proves to be effective both in cases with more samples than features and  
495 vice versa. The reduction in computation time is clear, for all the benchmark databases described, and is  
496 particularly attractive for high-dimensional datasets. Altogether, our feature selection approach U2FS,  
497 based on the utility metric, and with the binary or the RBF kernel with  $\hat{\sigma}^2$  is recommended due to its fast  
498 performance and its interpretability.

499 Additionally, the performance of U2FS is comparable to the state-of-the-art, as shown in Table 5. In  
500 this table, the performance of U2FS (RBF kernel and  $\hat{\sigma}^2$ , with the utility metric) is compared to that of  
501 RJGSC, given its consistent good results for different datasets when contrasted against the state-of-the-art.  
502 It is clear that terms of accuracy, both for 10% of the features and for the maximal value of achieved,  
503 U2FS obtains similar results to RJGSC. These results confirm the relevance of U2FS, in particular when  
504 taking into account its lower complexity. While RJGSC requires the manual tuning of extra parameters,  
505 similar to other algorithms in the state-of-the-art, U2FS tunes its parameters automatically. Hence, the  
506 application of the method is straightforward for the users. Additionally, similar to SAMM-FS and SOGFS,  
507 the RJGSC method performs manifold learning and feature selection simultaneously, iteratively adapting  
508 both steps to achieve optimal results. It is due to this that the achievement of comparable results is  
509 even more relevant, since U2FS is based on a greedy approach. Nevertheless, for these methods U2FS  
510 does not present as a competitor in terms of accuracy, but in terms of simplicity. The stages of higher  
511 complexity in U2FS, previously defined as  $O(N^3 + d^3)$ , are shared by most of the algorithms in the  
512 state-of-the-art. However, on top of these eigendecompositions and matrix inversions, the algorithms in  
513 the literature require a number of iterations in the optimization process that U2FS avoids. Additionally,  
514 U2FS is the only algorithm proposed based on a greedy approach, and therefore, the only one for which  
515 the computation time scales linearly with the amount of features selected.

516 The current state-of-the-art of unsupervised spectral feature selectors applies the stages of manifold  
517 learning and subset selection simultaneously, which can lead to optimal results. In a field that gets more  
518 and more complex and goes far from applicability, U2FS is presented as a quick solution for a sequential  
519 implementation of both stages of SSFS algorithms, yet achieving comparable results to the state-of-the-art.  
520 Being a greedy method, the utility metric cannot be applied simultaneously to the manifold learning and  
521 subset selection stages. However, other sequential algorithms from the state-of-the-art could consider  
522 the use of utility for subset selection, instead of the current sparsity-inducing techniques. One of the  
523 most direct applications could be the substitution of group-LASSO for group-utility, in order to perform  
524 selections of groups of features as proposed by Bertrand (2018). This can be of interest in cases where the  
525 relations between features are known, such as in channel selection (Narayanan and Bertrand, 2020) or in  
526 multi-modal applications (Zhao et al., 2015).

## 527 CONCLUSION

528 This work presents a new method for unsupervised feature selection based on manifold learning and  
529 sparse regression. The main contribution of this paper is the formulation of the utility metric in the field  
530 of spectral feature selection, substituting other sparse regression methods that require more computational  
531 resources. This method, being a backward greedy approach, has been proven to obtain comparable  
532 results to the state-of-the-art methods with analogous embedding approaches, yet at considerably reduced  
533 computational load. The method shows consistently good results in different applications, from images  
534 to text and sound data; and it is broadly applicable to problems of any size: using more features than  
535 samples or vice versa.

536 Furthermore, aiming to show the applicability of U2FS to data presenting non-linearities, the proposed  
537 approach has been evaluated in simulated data, considering both a binary and an RBF kernel embedding.  
538 Given the sensitivity of the RBF kernel to high-dimensional spaces, a new approximation of the RBF  
539 kernel parameter was proposed, which does not require further tuning around the value obtained. The

540 proposed approximation outperforms the rule-of-thumb widely used in the literature in most of the  
541 scenarios presented. Nevertheless, in terms of feature selection, the utility metric is robust against the  
542 embedding.

543 U2FS is proposed as a non-parametric efficient algorithm, which does not require any manual tuning  
544 or special knowledge from the user. Its simplicity, robustness and accuracy open a new path for structure  
545 sparsity-inducing feature selection methods, which can benefit from this quick and efficient technique.

## 546 REFERENCES

- 547 Aggarwal, C. C., Hinneburg, A., and Keim, D. A. (2001). On the surprising behavior of distance metrics  
548 in high dimensional space. In *International conference on database theory*, pages 420–434. Springer.
- 549 Alzate, C. and Suykens, J. A. (2008). Multiway spectral clustering with out-of-sample extensions through  
550 weighted kernel pca. *IEEE transactions on pattern analysis and machine intelligence*, 32(2):335–347.
- 551 Belkin, M. and Niyogi, P. (2002). Laplacian eigenmaps and spectral techniques for embedding and  
552 clustering. In *Advances in neural information processing systems*, pages 585–591.
- 553 Bertrand, A. (2018). Utility metrics for assessment and subset selection of input variables for linear  
554 estimation [tips & tricks]. *IEEE Signal Processing Magazine*, 35(6):93–99.
- 555 Biggs, N., Biggs, N. L., and Norman, B. (1993). *Algebraic graph theory*, volume 67. Cambridge university  
556 press.
- 557 Cai, D., Zhang, C., and He, X. (2010). Unsupervised feature selection for multi-cluster data. In  
558 *Proceedings of the 16th ACM SIGKDD international conference on Knowledge discovery and data  
559 mining*, pages 333–342.
- 560 Chung, F. R. and Graham, F. C. (1997). *Spectral graph theory*. Number 92. American Mathematical Soc.
- 561 Couvreur, C. and Bresler, Y. (2000). On the optimality of the backward greedy algorithm for the subset  
562 selection problem. *SIAM Journal on Matrix Analysis and Applications*, 21(3):797–808.
- 563 Deng Cai, Chiyuan Zhang, X. H. (2020). Supervised/Unsupervised/Semi-supervised Feature Selection  
564 for Multi-Cluster/Class Data.
- 565 Gui, J., Sun, Z., Ji, S., Tao, D., and Tan, T. (2016). Feature selection based on structured sparsity: A  
566 comprehensive study. *IEEE transactions on neural networks and learning systems*, 28(7):1490–1507.
- 567 Guyon, I. and Elisseeff, A. (2003). An introduction to variable and feature selection. *Journal of machine  
568 learning research*, 3(Mar):1157–1182.
- 569 He, X., Cai, D., and Niyogi, P. (2006). Laplacian score for feature selection. In *Advances in neural  
570 information processing systems*, pages 507–514.
- 571 Hou, C., Nie, F., Li, X., Yi, D., and Wu, Y. (2013). Joint embedding learning and sparse regression: A  
572 framework for unsupervised feature selection. *IEEE Transactions on Cybernetics*, 44(6):793–804.
- 573 Hwang, S.-G. (2004). Cauchy’s interlace theorem for eigenvalues of hermitian matrices. *The American  
574 Mathematical Monthly*, 111(2):157–159.
- 575 Jiang, X., Zhang, L., Zhao, Q., and Albayrak, S. (2006). Ecg arrhythmias recognition system based  
576 on independent component analysis feature extraction. In *TENCON 2006-2006 IEEE Region 10  
577 Conference*, pages 1–4. IEEE.
- 578 Li, Z., Yang, Y., Liu, J., Zhou, X., and Lu, H. (2012). Unsupervised feature selection using nonnegative  
579 spectral analysis. In *Twenty-Sixth AAAI Conference on Artificial Intelligence*.
- 580 Lunga, D., Prasad, S., Crawford, M. M., and Ersoy, O. (2013). Manifold-learning-based feature extraction  
581 for classification of hyperspectral data: A review of advances in manifold learning. *IEEE Signal  
582 Processing Magazine*, 31(1):55–66.
- 583 Maindonald, J. et al. (2007). Pattern recognition and machine learning. *Journal of Statistical Software*,  
584 17(b05).
- 585 Narayanan, A. M. and Bertrand, A. (2020). Analysis of miniaturization effects and channel selection  
586 strategies for eeg sensor networks with application to auditory attention detection. *IEEE Transactions  
587 on Biomedical Engineering*, 67(1):234–244.
- 588 Ng, A. Y., Jordan, M. I., and Weiss, Y. (2002). On spectral clustering: Analysis and an algorithm. In  
589 *Advances in neural information processing systems*, pages 849–856.
- 590 Nie, F., Zhu, W., and Li, X. (2019). Structured graph optimization for unsupervised feature selection.  
591 *IEEE Transactions on Knowledge and Data Engineering*.
- 592 Reynolds, B. E. (1980). Taxicab geometry. *Pi Mu Epsilon Journal*, 7(2):77–88.
- 593 Szurley, J., Bertrand, A., and Moonen, M. (2012). Efficient computation of microphone utility in a

- 594 wireless acoustic sensor network with multi-channel wiener filter based noise reduction. In *2012 IEEE*  
595 *International Conference on Acoustics, Speech and Signal Processing (ICASSP)*, pages 2657–2660.  
596 IEEE.
- 597 Szurley, J., Bertrand, A., Ruckebusch, P., Moerman, I., and Moonen, M. (2014). Greedy distributed node  
598 selection for node-specific signal estimation in wireless sensor networks. *Signal Processing*, 94:57–73.
- 599 Tharwat, A., Hassanien, A. E., and Elnaghi, B. E. (2017). A ba-based algorithm for parameter optimization  
600 of support vector machine. *Pattern Recognition Letters*, 93:13–22.
- 601 Tsironis, S., Sozio, M., Vazirgiannis, M., and Poltechnique, L. (2013). Accurate spectral clustering for  
602 community detection in mapreduce. In *Advances in Neural Information Processing Systems (NIPS)*  
603 *Workshops*. Citeseer.
- 604 Varon, C., Alzate, C., and Suykens, J. A. (2015). Noise level estimation for model selection in kernel pca  
605 denoising. *IEEE transactions on neural networks and learning systems*, 26(11):2650–2663.
- 606 Verleysen, M. and François, D. (2005). The curse of dimensionality in data mining and time series  
607 prediction. In *International Work-Conference on Artificial Neural Networks*, pages 758–770. Springer.
- 608 Von Luxburg, U. (2007). A tutorial on spectral clustering. *Statistics and computing*, 17(4):395–416.
- 609 Wold, S., Esbensen, K., and Geladi, P. (1987). Principal component analysis. *Chemometrics and intelligent*  
610 *laboratory systems*, 2(1-3):37–52.
- 611 Yan, S., Xu, D., Zhang, B., Zhang, H.-J., Yang, Q., and Lin, S. (2006). Graph embedding and extensions:  
612 A general framework for dimensionality reduction. *IEEE transactions on pattern analysis and machine*  
613 *intelligence*, 29(1):40–51.
- 614 Yang, Y., Shen, H. T., Ma, Z., Huang, Z., and Zhou, X. (2011). L2, 1-norm regularized discriminative  
615 feature selection for unsupervised. In *Twenty-Second International Joint Conference on Artificial*  
616 *Intelligence*.
- 617 Yin, S. and Yin, J. (2016). Tuning kernel parameters for svm based on expected square distance ratio.  
618 *Information Sciences*, 370:92–102.
- 619 Zhang, R., Nie, F., Wang, Y., and Li, X. (2019). Unsupervised feature selection via adaptive multimeasure  
620 fusion. *IEEE transactions on neural networks and learning systems*, 30(9):2886–2892.
- 621 Zhao, L., Hu, Q., and Wang, W. (2015). Heterogeneous feature selection with multi-modal deep neural  
622 networks and sparse group lasso. *IEEE Transactions on Multimedia*, 17(11):1936–1948.
- 623 Zhao, Z. and Liu, H. (2007). Spectral feature selection for supervised and unsupervised learning. In  
624 *Proceedings of the 24th international conference on Machine learning*, pages 1151–1157.
- 625 Zhu, X., Li, X., Zhang, S., Ju, C., and Wu, X. (2016). Robust joint graph sparse coding for unsupervised  
626 spectral feature selection. *IEEE transactions on neural networks and learning systems*, 28(6):1263–  
627 1275.